Ref: Ro J Stomatol. 2022;68(3)
DOI: 10.37897/RJS.2022.3.3

Comparative analysis of the experimental dilation of some materials used in the manufacture of physiognomic fixed prosthetic restorations

Mirel Stoian-Albulescu[1], Doina Lucia Ghergic[2], Costin Coman[2], Raluca-Monica Comaneanu[2], Oana Botoaca[2], Dan Nicolae Patroi[2]

[1] Doctoral School of Dental Medicine, "Titu Maiorescu" University, Bucharest, Romania
[2] Faculty of Dental Medicine, "Titu Maiorescu" University, Bucharest, Romania

ABSTRACT

Aim of the study was the comparative analysis of the experimental dilation of some materials used in the fabrication of physiognomic fixed prosthetic restorations.
Material and methods. 3 biomaterials used in the fabrication of physiognomic fixed prosthetic restorations, pressed ceramic IPS e.max Press Ivoclar Vivadent, WhitePeaks Copra Smile (ZrO2, 600 MPa) and WhitePeaks Copra Supreme (ZrO2, 1100 MPa) were comparatively analyzed.
The temperature increase was carried out from 20^{O}C to 400^{O}C, with the speed of 2 degrees/minute in a dilatometer. The repetition of the heating was done 2 times, with a 30-minute break between attempts.
Results. The smallest expansion occurred for the e.max sample, followed by Zr600 and Zr1100.
Conclusions. The present study demonstrated the production of a thermal expansion at the level of pressed ceramics and biomaterials based on zirconium dioxide upon experimental heating in the range of 20-400^{O}C in dilatometer. Subjecting pressed ceramic or zirconium dioxide prosthetic restorations to high temperatures during the clinical-technical phases of occlusal processing/adaptation without adequate cooling may introduce residual thermal stresses into the material structure, which may subsequently lead to cracking of the prosthetic restorations under stress conditions determined by masticatory forces.

Keywords: thermal expansion, dilatometer, physiognomic materials, prosthetic restorations

INTRODUCTION

Thermal expansion [1-4], is a phenomenon of increasing the macroscopic dimensions of the material upon heating, due to the thermal vibrations of the crystalline network (or of the constituent particles of the amorphous state). At any temperature, the atoms of the solid vibrate with amplitudes of the order of 10^{-9} cm and the frequency of approx. 10^{13} Hz. When the temperature increases, there is a change in the distances between the atoms, resulting in a change in the macroscopic dimensions of the body. It was found experimentally that the relationship between the variation in linear dimensions and the variation in temperature ΔT is given by a relationship [5] of the type:

$$\Delta l = \alpha \cdot l_0 \cdot \Delta T$$

where: α is the thermal expansion coefficient, being a material constant

$$\alpha = \frac{l}{l_0} \cdot \frac{\Delta l}{\Delta T}$$

i.e. α represents the relative change in material length at a 1 K temperature rise.

Corresponding author:
Raluca-Monica Comaneanu
E-mail: monica.comaneanu@prof.utm.ro

Article History:
Received: 22 August 2022
Accepted: 29 August 2022

Surface expansion ΔS and volume expansion ΔV were similarly defined, i.e.:

$$\Delta S = \beta \cdot S_0 \cdot \Delta T$$

$$\Delta V = \gamma \cdot V_0 \cdot \Delta T$$

where $\beta \approx 2\alpha$ and $\gamma \approx 3\alpha$ are the coefficients of surface expansion and volume expansion, respectively.

The explanation of the phenomenon of thermal expansion can only be given in an anharmonic approximation of the oscillation energy of atoms. For this we will note that, since the atoms in the network vibrate continuously, the dimensions of the bodies are not given by the instantaneous distances between the atoms, but only by the average distances.

Thermal analysis [6,7] is part of the group of methods by which the physical and chemical properties of some substances (compounds) are determined, depending on the variation in temperature or time, based on the thermal effects that accompany the transformations that take place in the sample in heating, cooling, isothermal holding time, etc. These methods are called "thermoanalytical methods", and the Figures obtained from the determinations are called thermograms or "thermal analysis curves".

The aim of the present study was the comparative analysis of the experimental dilation of some materials used in the fabrication of physiognomic fixed prosthetic restorations.

MATERIAL AND METHODS

3 biomaterials used in the fabrication of physiognomic fixed prosthetic restorations, pressed ceramic IPS e.max Press Ivoclar Vivadent, WhitePeaks Copra Smile (ZrO_2, 600 MPa) and WhitePeaks Copra Supreme (ZrO_2, 1100 MPa) were comparatively analyzed.

From each material, a parallelepiped sample was made in the dental laboratory, with a length of 40 mm and a section side of 4 mm. The e.max sample was obtained by pressing, and the Zr600 and Zr1200 samples were obtained by milling into ZrO_2 discs and sintering according to the manufacturers' specifications.

The dilatometer on which the dilatometric curves were quantified is a vertical, high-temperature one, Unitherm 1161V model, from the Thermophysical Testing Laboratory of the Faculty of Materials Science and Engineering, Polytechnic University of Bucharest.

This apparatus is fully computerized and is intended to measure linear variations of samples due to thermal changes, according to ASTM E-228 [8].

In the present study, the temperature increase was carried out from 20ºC to 400ºC, with the speed of 2 degrees/minute. Each sample was kept at the maximum set temperature for 5 minutes, after which it cooled down controlled at the same rate. The repetition of the heating was done 2 times, with a 30-minute break between attempts.

The diagrams provided by the dilatometer software were compared with each other. Based on the diagrams, the software calculated the coefficients of linear thermal expansion specific to each material, which were later used to calculate the length L of each sample at a given temperature, but also the difference ΔL between the length after heating and the initial length.

RESULTS

The Figure 1 shows the dependence of expansion on temperature in the two heating/cooling cycles of the e.max material. Red shows the first heating/cooling cycle, and pink the second cycle. The Figure have a stepwise evolution as the heating is done step by step under computer control. We note that the expansion produced in the first heating/cooling cycle was slightly higher than in the second cycle. The phenomenon can be explained by a stabilization produced at the material level after the first cycle.

The Figure 2 shows the average of the thermal expansion produced during the two cycles, the average of the instantaneous thermal expansion coefficient and the average of the linear thermal expansion coefficient. While the first two have a linear, constantly increasing evolution, the third initially has a more accelerated growth, followed by a slow growth.

The Figure 3 shows the dependence of expansion on temperature in the two heating/cooling cycles for Zr600 material. As with the e.max, the first heating/cooling cycle is shown in red, and the second cycle in pink. The Figures also have a gradual evolution because the heating is done step by step, under computer control.

We note that the expansion produced in the first heating/cooling cycle was slightly higher than in the second cycle. The phenomenon can also be explained by a stabilization produced at the material level after the first heating/cooling cycle.

The Figure 4 shows the average of the thermal expansion produced during the two cycles, the average of the instantaneous thermal expansion coefficient and the average of the linear thermal expansion coefficient. While the first two have a linear, constantly increasing evolution, the third initially has a more accelerated growth, followed by a slow growth.

The Figure 5 shows the dependence of expansion on temperature in the two heating/cooling cycles for Zr1100 material. As with the e.max and Zr600, red shows the first heating/cooling cycle and pink the second cycle. The Figures also have a gradual evolu-

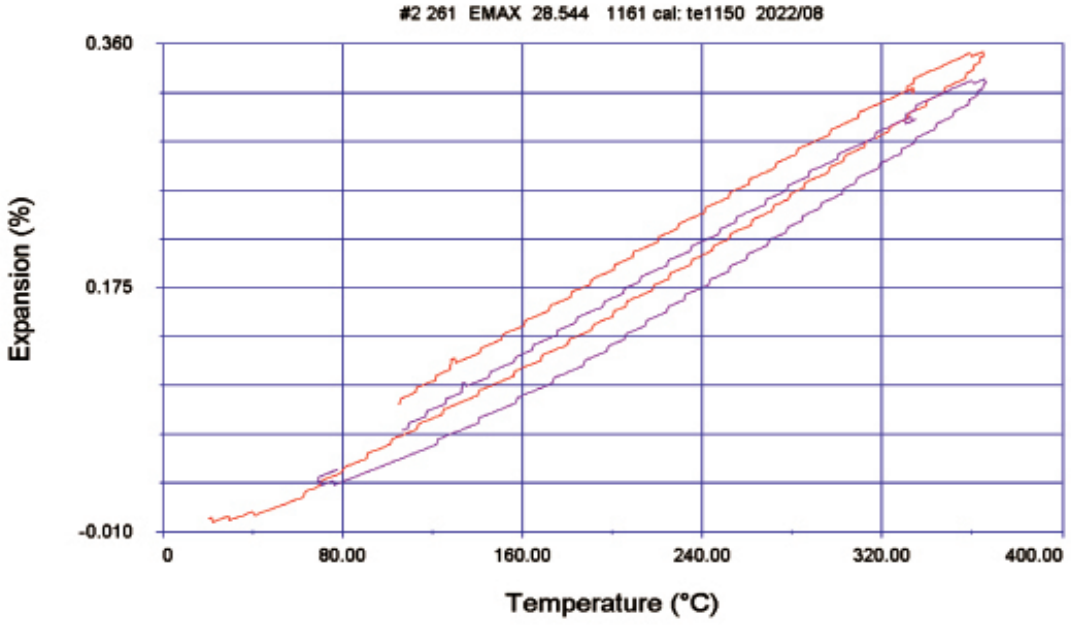

FIGURE 1. Graphic representation of the two heating/cooling cycles for e.max

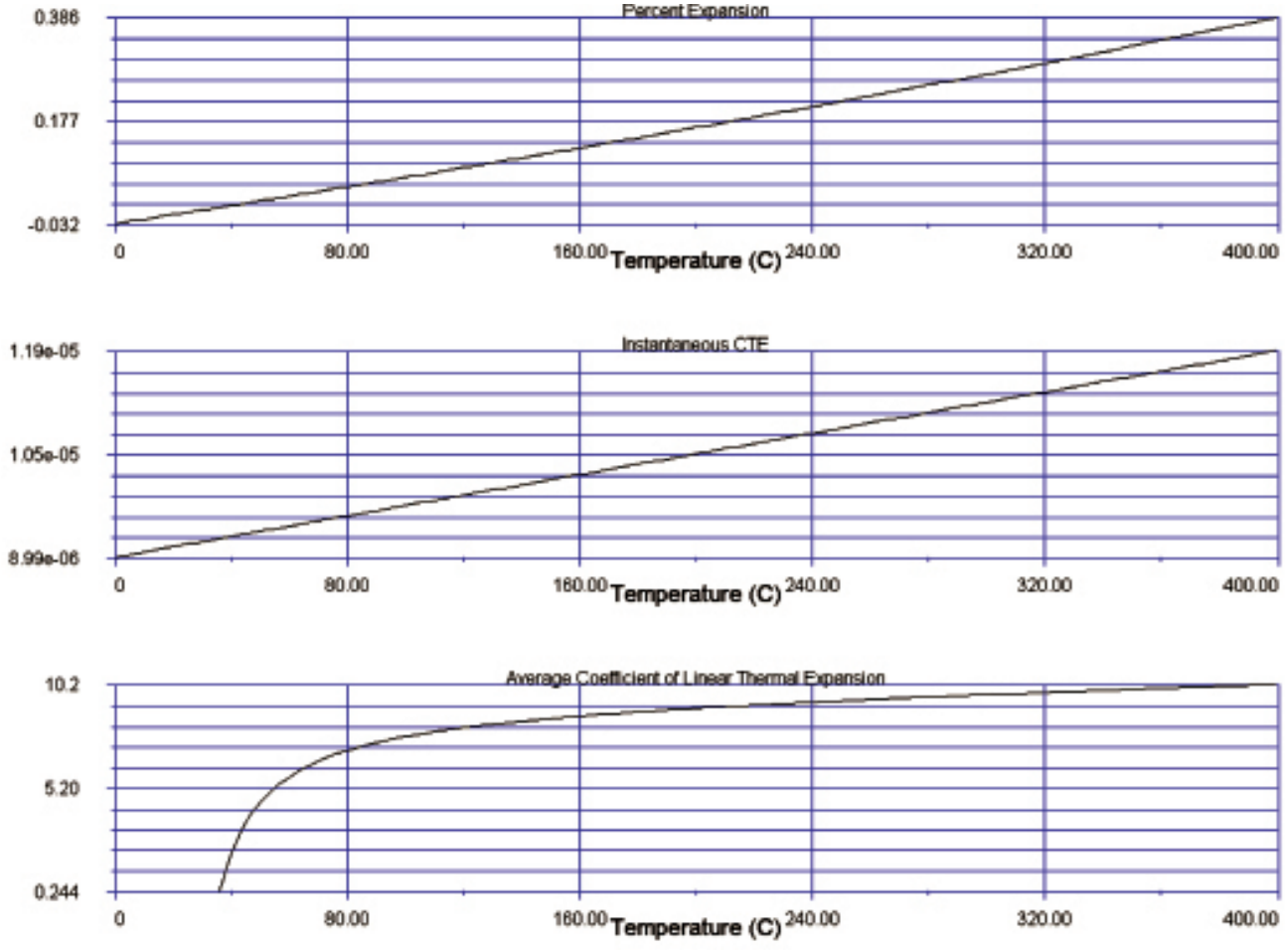

FIGURE 2. A) Thermal expansion average produced during the two cycles for e.max (top), B) The average of instantaneous thermal expansion coefficient for e.max (middle) and C) The average of linear thermal expansion coefficient for e.max (down)

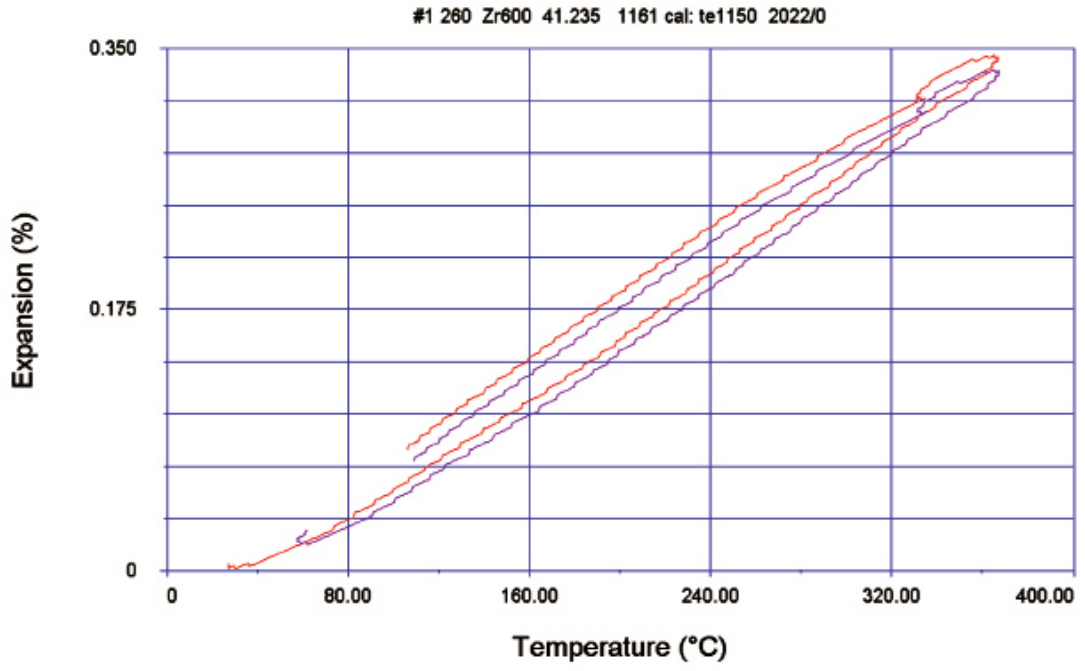

FIGURE 3. Graphic representation of the two heating/cooling cycles for Zr600

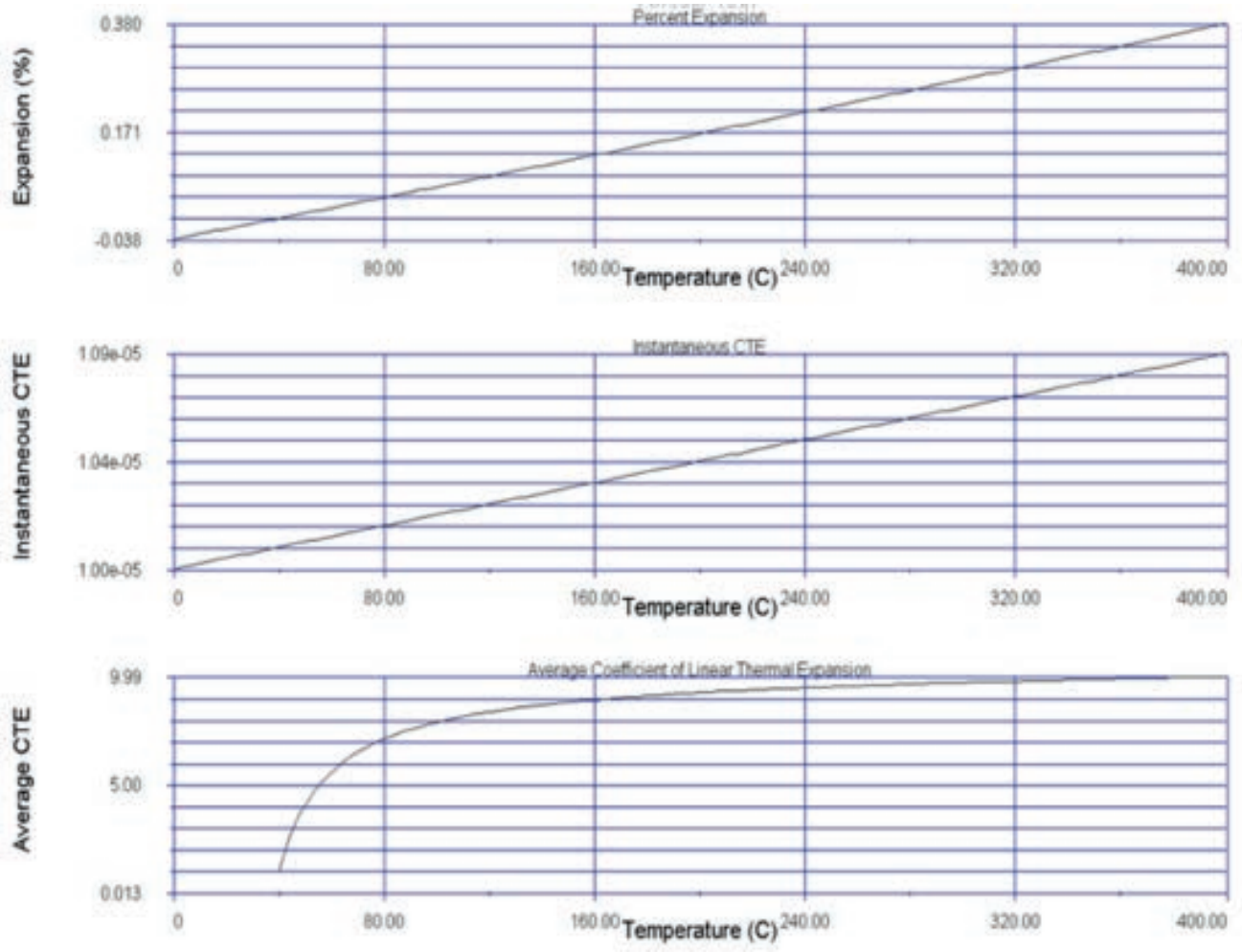

FIGURE 4. A) Thermal expansion average produced during the two cycles for Zr600 (top), B) The average of instantaneous thermal expansion coefficient for Zr600 (middle) and C) The average of linear thermal expansion coefficient for Zr600

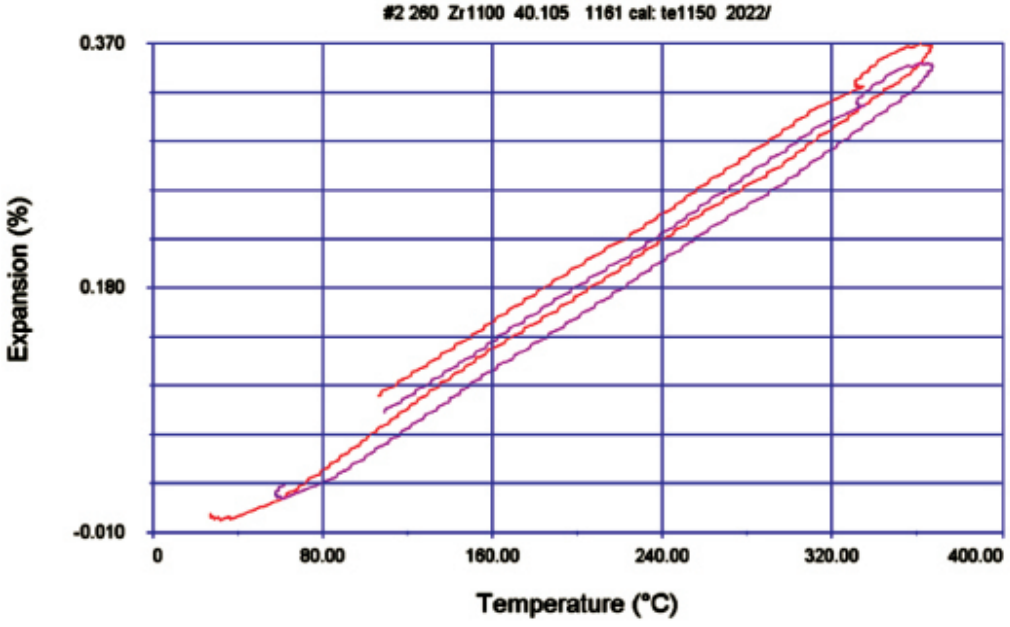

FIGURE 5. Graphic representation of the two heating/cooling cycles for Zr1100

tion because the heating is done step by step, under computer control. We note that the expansion produced in the first heating/cooling cycle was slightly higher than in the second cycle. The phenomenon can also be explained by a stabilization produced at the material level after the first heating/cooling cycle.

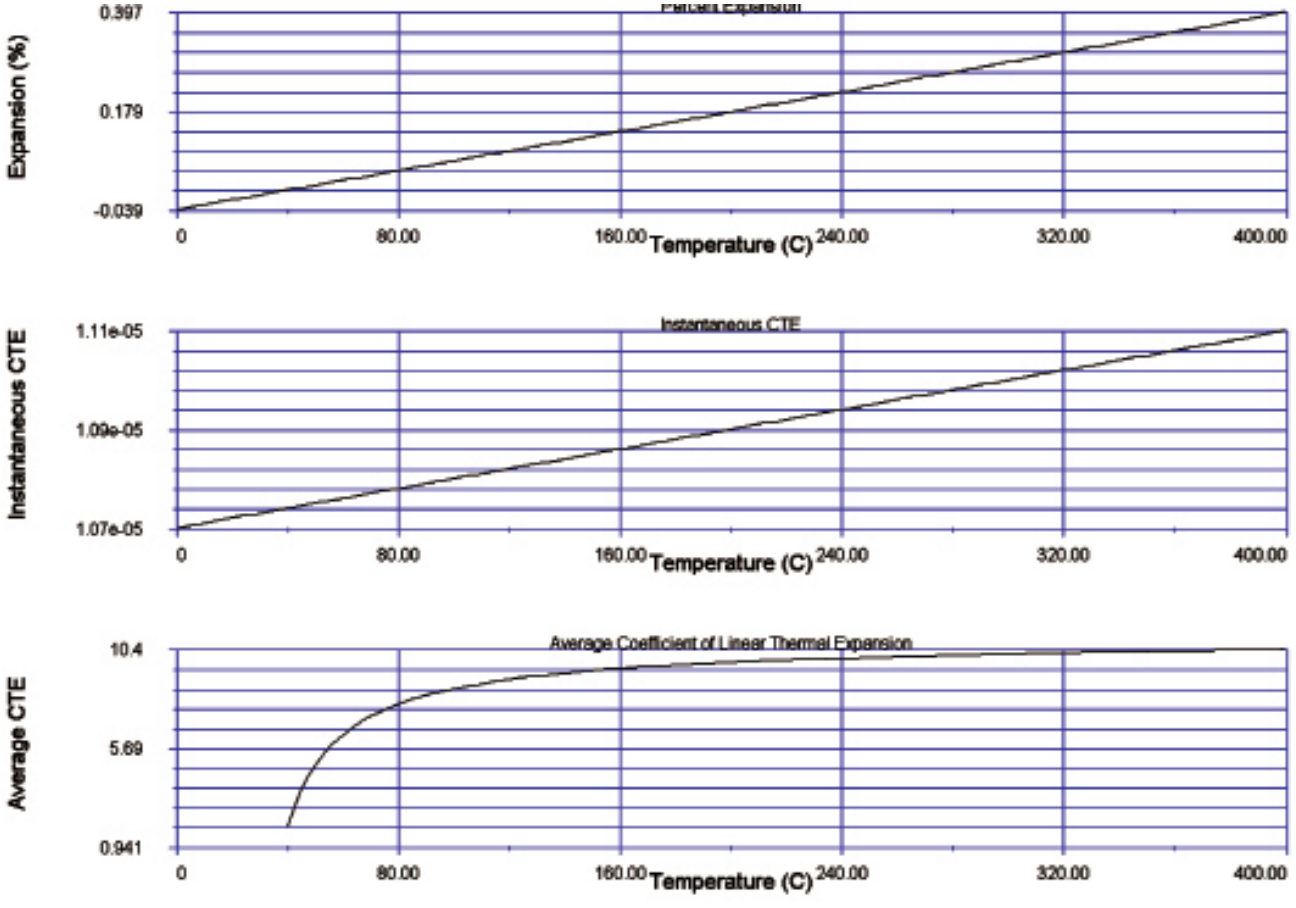

FIGURE 6. A) Thermal expansion average produced during the two cycles for Zr1100 (top), B) The average of instantaneous thermal expansion coefficient for Zr1100 (middle) and C) The average of linear thermal expansion coefficient for Zr1100

The Figure 6 shows the average of the thermal expansion produced during the two cycles, the average of the instantaneous thermal expansion coefficient and the average of the linear thermal expansion coefficient. While the first two have a linear, constantly increasing evolution, the third initially has a more accelerated growth, followed by a slow growth.

Based on the Figures, it was possible to calculate the coefficients of linear thermal expansion for the 3 studied materials. The values of the respective coefficients are recorded in table 1.

TABLE 1. Linear thermal expansion coefficients for the 3 studied materials

Material	e.max	Zr600	Zr1100
Coefficient of linear thermal expansion, $\times 10^{-6}$ [degree^{-1}]	9.725	10.227	10.784

Table 2 shows the average lengths of the samples during the two heating cycles from 10 to 10 degrees Celsius, as well as the size ΔL, which represents the value of the average expansion.

TABLE 2. The average size of the samples after the expansion produced at different temperatures and the ΔL value, which represents the value of the average expansion

Material / Temperature, °C	e.max		Zr600		Zr1100	
	L [mm]	ΔL [mm]	L [mm]	ΔL [mm]	L [mm]	ΔL [mm]
20	40.007780	0.007780	40.008182	0.008182	40.008627	0.008627
30	40.011670	0.011670	40.012272	0.012272	40.012941	0.012941
40	40.015560	0.015560	40.016363	0.016363	40.017254	0.017254
50	40.019450	0.019450	40.020454	0.020454	40.021568	0.021568
60	40.023340	0.023340	40.024545	0.024545	40.025882	0.025882
70	40.027230	0.027230	40.028636	0.028636	40.030195	0.030195
80	40.031120	0.031120	40.032726	0.032726	40.034509	0.034509
90	40.035010	0.035010	40.036817	0.036817	40.038822	0.038822
100	40.038900	0.038900	40.040908	0.040908	40.043136	0.043136
110	40.042790	0.042790	40.044999	0.044999	40.047450	0.047450
120	40.046680	0.046680	40.049090	0.049090	40.051763	0.051763
130	40.050570	0.050570	40.053180	0.053180	40.056077	0.056077
140	40.054460	0.054460	40.057271	0.057271	40.060390	0.060390
150	40.058350	0.058350	40.061362	0.061362	40.064704	0.064704
160	40.062240	0.062240	40.065453	0.065453	40.069018	0.069018
170	40.066130	0.066130	40.069544	0.069544	40.073331	0.073331
180	40.070020	0.070020	40.073634	0.073634	40.077645	0.077645
190	40.073910	0.073910	40.077725	0.077725	40.081958	0.081958
200	40.077800	0.077800	40.081816	0.081816	40.086272	0.086272
210	40.081690	0.081690	40.085907	0.085907	40.090586	0.090586
220	40.085580	0.085580	40.089998	0.089998	40.094899	0.094899
230	40.089470	0.089470	40.094088	0.094088	40.099213	0.099213
240	40.093360	0.093360	40.098179	0.098179	40.103526	0.103526
250	40.097250	0.097250	40.102270	0.102270	40.107840	0.107840
260	40.101140	0.101140	40.106361	0.106361	40.112154	0.112154
270	40.105030	0.105030	40.110452	0.110452	40.116467	0.116467
280	40.108920	0.108920	40.114542	0.114542	40.120781	0.120781
290	40.112810	0.112810	40.118633	0.118633	40.125094	0.125094
300	40.116700	0.116700	40.122724	0.122724	40.129408	0.129408
310	40.120590	0.120590	40.126815	0.126815	40.133722	0.133722
320	40.124480	0.124480	40.130906	0.130906	40.138035	0.138035
330	40.128370	0.128370	40.134996	0.134996	40.142349	0.142349
340	40.132260	0.132260	40.139087	0.139087	40.146662	0.146662
350	40.136150	0.136150	40.143178	0.143178	40.150976	0.150976
360	40.140040	0.140040	40.147269	0.147269	40.155290	0.155290
370	40.143930	0.143930	40.151360	0.151360	40.159603	0.159603
380	40.147820	0.147820	40.155450	0.155450	40.163917	0.163917
390	40.151710	0.151710	40.159541	0.159541	40.168230	0.168230
400	40.155600	0.155600	40.163632	0.163632	40.172544	0.172544

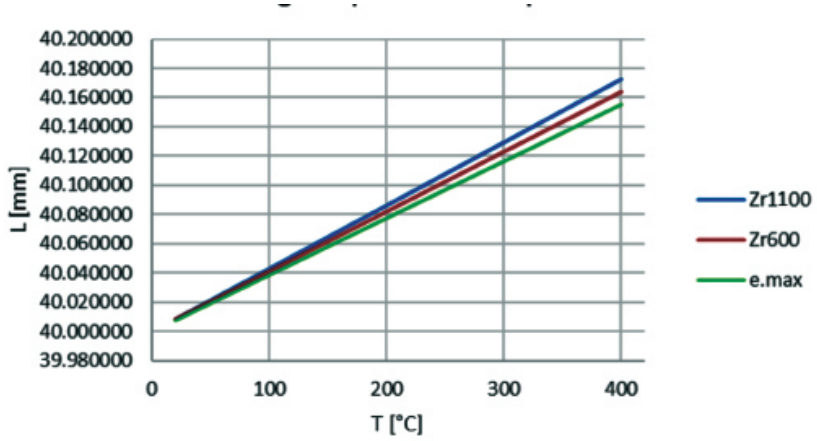

FIGURE 7. Evolution of the length of the samples during heating

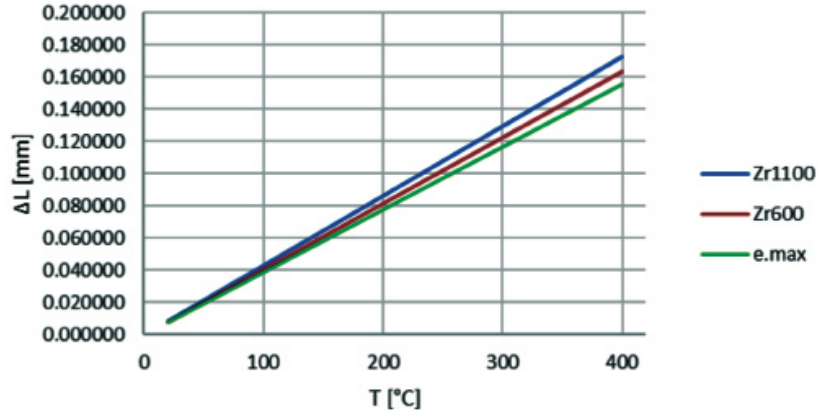

FIGURE 8. Evolution of sample expansion during heating

The evolution of the length of the samples during heating (Figure 7) and the evolution of the expansion of the samples during heating (Figure 8) were graphically illustrated comparatively.

From the analysis of the Figures, it is visible that the smallest expansion occurred for the e.max sample, followed by Zr600 and Zr1100.

DISCUSSIONS

In the oral environment, the biomaterials used for the direct or indirect restoration of the functions of the dento-maxillary apparatus are subject to particular conditions – variations in pH, temperature and pressure [9-19]. The pH variations are given by the food/drinks ingested, by the eventual reflux of gastric contents [20], but also by the presence of varied microbial flora. The temperature in the oral environment varies when cold or hot food/drinks are ingested, and the occlusal pressures during mastication stress the masticatory units and the supporting alveolar bone through the dento-periodontal ligaments.

Ceramic materials exhibit increased hardness, abrasion resistance, reduced density compared to metallic alloys, and dimensional stability [21] up to the sintering temperature.

Systematic reviews evaluating clinical trials reported a higher incidence of failure in zirconium dioxide-based restorations compared to metal framework restorations [22]. The main factor that produced the chipping of the material seems to be the development of internal stresses, which zirconium dioxide, as a brittle material, is less able to compensate than the classical form of the metal substrate. Therefore, it is important to keep the overall stress state of the restorations as low as possible [23]. The general stress state includes the sum of the stresses that appear externally, as a result of performing the functions of the dento-maxillary apparatus (incision, trituration and pressing) and internally, due to residual stresses [23]. These internal residual stresses are primarily thermal stresses that are applied to the restoration during manufacture and "stored" in its structure during cooling [24].

Similar to our research, the tests performed by Preis et al. [25] on zirconia and a glass-ceramic material, which were subjected to heating up to 55°C, demonstrated that ceramics and zirconia exhibit coefficients of expansion at moderate temperature increases relative to sintering temperatures.

CONCLUSIONS

The present study demonstrated the production of a thermal expansion at the level of pressed ceramics and biomaterials based on zirconium dioxide upon experimental heating in the range of 20-400°C in dilatometer.

Among the 3 materials analyzed comparatively, within the limits of this study, e.max presented the lowest coefficient of expansion, and Zr1100 had the highest coefficient of expansion.

Subjecting pressed ceramic or zirconium dioxide prosthetic restorations to high temperatures during the clinical-technical phases of occlusal processing/adaptation without adequate cooling may introduce residual thermal stresses into the material structure, which may subsequently lead to cracking of the prosthetic restorations under stress conditions determined by masticatory forces.

Conflict of interest: none declared
Financial support: none declared

REFERENCES

1. Liu ZK, Shang SL, Wang Y. Fundamentals of Thermal Expansion and Thermal Contraction. *Materials (Basel).* 2017 Apr 14;10(4):410. doi: 10.3390/ma10040410.
2. Pluta Z. Thermal expansion of Solids. *J Modern Physic.* 2012;3(08):793-802. doi: 10.4236/jmp.2012.38104.
3. Wang X, Bai X, Xiao W, Liu Y, Li X, Wang J, Peng C, Wang L, Wang X. Calculation of Thermal Expansion Coefficient of Rare Earth Zirconate System at High Temperature by First Principles. *Materials (Basel).* 2022 Mar 18;15(6):2264. doi: 10.3390/ma15062264.
4. Yang Y, Lin Z, Li R, Li Y, Liu W, Tian S, Zhu K, Long L. Thermal expansion coefficient of monolayer MoS_2 determined using temperature-dependent Raman spectroscopy combined with finite element simulations. *Microstructures*. 2021;1:2021002. doi:10.20517/microstructures.2021.02
5. Rath J, Pospisil, Z et al. Jemnakeramika-metodikaměřeni a zkousek. Praha: SNTL/Alfa, 1988.
6. https://termoanalitic.wordpress.com/2011/02/04/definirea-unor-metode-de-analiza-termica/
7. https://www.scribd.com/doc/124041178/Analiza-Termica
8. https://www.astm.org/e0228-17.html
9. Read E, Curtis MA, Neves JF. The role of oral bacteria in inflammatory bowel disease. Nat Rev Gastroenterol Hepatol. 2021 Oct;18(10):731-42. doi: 10.1038/s41575-021-00488-4. Epub 2021 Aug 16. PMID: 34400822.
10. Sedghi L, DiMassa V, Harrington A, Lynch SV, Kapila YL. The oral microbiome: Role of key organisms and complex networks in oral health and disease. *Periodontol 2000.* 2021 Oct;87(1):107-31. doi: 10.1111/prd.12393. PMID: 34463991; PMCID: PMC8457218.
11. Ciesielska A, Kusiak A, Ossowska A, Grzybowska ME. Changes in the Oral Cavity in Menopausal Women-A Narrative Review. *Int J Environ Res Public Health.* 2021 Dec 27;19(1):253. doi: 10.3390/ijerph19010253. PMID: 35010513; PMCID: PMC8750983.
12. Lin D, Yang L, Wen L, Lu H, Chen Q, Wang Z. Crosstalk between the oral microbiota, mucosal immunity, and the epithelial barrier regulates oral mucosal disease pathogenesis. *Mucosal Immunol.* 2021 Nov;14(6):1247-58. doi: 10.1038/s41385-021-00413-7. Epub 2021 May 26. PMID: 34040155.
13. Peng X, Cheng L, You Y, Tang C, Ren B, Li Y, Xu X, Zhou X. Oral microbiota in human systematic diseases. *Int J Oral Sci.* 2022 Mar 2;14(1):14. doi: 10.1038/s41368-022-00163-7. PMID: 35236828; PMCID: PMC8891310.
14. Bechir F, Pacurar M, Tohati A, Bataga SM. Comparative Study of Salivary pH, Buffer Capacity, and Flow in Patients with and without Gastroesophageal Reflux Disease. *Int J Environ Res Public Health.* 2021 Dec 25;19(1):201. doi: 10.3390/ijerph19010201. PMID: 35010461; PMCID: PMC8750732.
15. Kukreja P, Hugar SM, Hallikerimath S, Sogi S, Badakar C, Thakkar P. Evaluation of the Effect of Fixed and Removable Appliances on Salivary Parameters (Salivary Flow Rate pH and Buffering Capacity) in Children Aged 5-12 Years: An In Vivo Study. *Int J Clin Pediatr Dent*. 2021 Nov-Dec;14(6):774-8. doi: 10.5005/jp-journals-10005-2066. PMID: 35110870; PMCID: PMC8783221.
16. Matuq Badri S, Felemban EH, Alnajjar GK, Alotaibi FM, Aljahdali ST, Maher YA, Fathi A. Effectiveness of probiotic lozenges and Chlorhexidine mouthwash on plaque index, salivary pH, and Streptococcus mutans count among school children in Makkah, Saudi Arabia. *Saudi Dent J.* 2021 Nov;33(7):635-641. doi: 10.1016/j.sdentj.2020.05.006. Epub 2020 Jun 3. PMID: 34803312; PMCID: PMC8589601.
17. Qadeer S, Özcan M, Edelhoff D, Van Pelt H. Accuracy. Reliability and Clinical Implications of Static Compared to Quantifiable Occlusal Indicators. *Eur J Prosthodont Restor Dent.* 2021 Aug 31;29(3):130-41. doi: 10.1922/EJPRD_2202Qadeer12. PMID: 33508180.
18. Kim YJ, Ko KH, Huh YH, Cho LR, Park CJ. Initial Change in the Occlusal Force and Occlusal Contact Area Following Single Molar Implant Restoration. *Int J Oral Maxillofac Implants.* 2021 Nov-Dec; 36(6):1139-46. doi: 10.11607/jomi.8962. PMID: 34919612.
19. Sana S, Kondody RT, Talapaneni AK, Fatima A, Bangi SL. Occlusal stress distribution in the human skull with permanent maxillary first molar extraction: A 3-dimensional finite element study. *Am J Orthod Dentofacial Orthop.* 2021 Oct;160(4):552-559. doi: 10.1016/j.ajodo.2020.05.022. Epub 2021 Jul 14. PMID: 34274197.
20. Sikavi DR, Cai JX, Leung R, Carroll TL, Chan WW. Impaired Proximal Esophageal Contractility Predicts Pharyngeal Reflux in Patients With Laryngopharyngeal Reflux Symptoms. *Clin Transl Gastroenterol.* 2021 Oct 1;12(10):e00408. doi: 10.14309/ctg.0000000000000408. PMID: 34597279; PMCID: PMC8487779.
21. Pop GhT, Chirita M, Rostami M. Materiale Bioceramice. Iasi: Tehnopres, 2003.
22. Pjetursson BE, Sailer I, Makarov NA, Zwahlen M, Thoma DS. All-ceramic or metal-ceramic tooth-supported fixed dental prostheses (FDPs)? A systematic review of the survival and complication rates. Part II: Multiple-unit FDPs. *Dental Mater.* 2015 Jun;31(6):624-39. doi: 10.1016/j.dental.2015.02.013.
23. Hensel J, Reise M, Liebermann A, Buser R, Stawarczyk B. Impact of multiple firings on thermal properties and bond strength of veneered zirconia restorations. *J Mech Behav Biomed Mater.* 2022 Apr;128:105134. doi: 10.1016/j.jmbbm.2022.105134. Epub 2022 Feb 17. PMID: 35196634.
24. Tholey MJ, Swain MV, Thiel N. Thermal gradients and residual stresses in veneered Y-TZP frameworks. *Dental Mater.* 2011 Nov;27(11):1102-10. doi: 10.1016/j.dental.2011.08.001.
25. Preis V, Grumser K, Schneider-Feyrer S, Behr M, Rosentritt M. Cycle-dependent in vitro wear performance of dental ceramics after clinical surface treatments. *J Mech Behav Biomed Mater.* 2016 Jan;53:49-58. doi: 10.1016/j.jmbbm.2015.08.009.